

Material Strategies for Black-to-Transmissive Window-Type Polymer Electrochromic Devices

Svetlana V. Vasilyeva,[†] Pierre M. Beaujuge,[†] Shujun Wang,[§] Joseph E. Babiarez,[§] Vincent W. Ballarotto,[‡] and John R. Reynolds^{*,†}

[†]The George and Josephine Butler Polymer Research Laboratory, Department of Chemistry, Center for Macromolecular Science and Engineering, University of Florida, Gainesville, Florida 32611-7200, United States

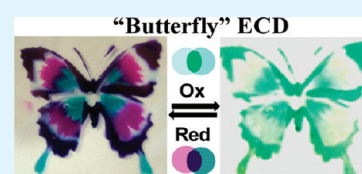
[§]BASF, Tarrytown, New York 10591, United States

[‡]Laboratory for Physical Sciences, University of Maryland, College Park, Maryland 20740, United States

S Supporting Information

ABSTRACT: Black-to-transmissive switching polymer electrochromic devices (ECDs) were designed using a set of spray-processable cathodically coloring polymers, a non-color-changing electroactive polymer poly(2,2,6,6-tetramethylpiperidinyloxy-4-yl methacrylate) (PTMA) as the charge-compensating counter electrode, and a highly conducting gel electrolyte (6.5 mS cm^{-1}). The color “black” was obtained by utilizing (1) individual copolymers absorbing across the visible spectrum, and (2) blends and bilayers of several polymer electrochromes with complementary spectral absorption. Neutral-state black and ink-like dark purple-blue (or “ink-black”) donor–acceptor (DA) copolymers composed of the electron-donor 3,4-propylenedioxythiophene (ProDOT) and the electron-acceptor 2,1,3-benzothiadiazole (BTD) building units, which possess relatively homogeneous absorption profiles across the visible spectrum, were chosen for their propensity to switch to transmissive states upon electrochemical oxidation. A blend of magenta and cyan polymers (PProDOT-(CH₂OEtHx)₂ and P(ProDOT-BTD-ProDOT), respectively) was produced with the goal of generating the same dark purple-blue color as that obtained with the “ink-black” DA copolymer. While the multi-polymer ECDs demonstrate high contrasts (up to 50%T), and switch from a saturated purple-blue color ($L^* = 32$, $a^* = 13$, $b^* = -46$) to a light green-blue transmissive state ($L^* = 83$, $a^* = -3$, $b^* = -6$), devices made with the DA electrochromic copolymers switch more than two times faster (0.7 s to attain 95% of the full optical change) than those involving the polymer blends (1.6 s), and exhibit more neutral achromatic colors ($L^* = 38$, $a^* = 5$, $b^* = -25$ for the colored state and $L^* = 87$, $a^* = -3$, $b^* = -2$ for the bleached state, correspondingly). The results obtained suggest that these materials should prove to be applicable in both transmissive- (window-type) and reflective-type ECDs.

KEYWORDS: electrochromism, conjugated polymer, electrochromic device



1. INTRODUCTION

In electrochromic (EC) systems, electrochemical redox reactions result in a reversible variation of transmitted/reflected light, inducing color changes in the electroactive material. Commercialization of EC materials in absorptive/transmissive and reflective-type electrochromic devices (ECDs), including residential, aircraft and automotive windows/roofs, wearable vision systems (goggles, helmets)^{1–3} and fabrics (camouflage, chameleonic Spandex),^{4,5} dimming mirrors, electronic tags, signage, and e-paper,^{6,7} requires that specific optical, electrochemical, and mechanical properties be attained. Recent research effort has been focused on the synthesis and characterization of electrochromic π -conjugated polymers (ECPs), and several important reasons for using polymeric electrochromes over their more traditional organic and inorganic counterparts, such as metallophthalocyanines, viologens, and inorganic metal oxides,^{1,8} have been emphasized. In particular, a wide range of saturated colors attainable via structural modification of the polymer backbone, high transmittance in the bleached states, fast and effective color modulation properties in combination with redox stability,

mechanical conformability and solution-processability make polymer electrochromes excellent candidates for ECDs.⁹

Following “color-mixing theory” principles, it is possible to obtain a full color palette, including black, when subtractive primary cyan, magenta, and yellow (CMY) colors and secondary red, yellow, and blue (RYB) colors are accessible. To be successfully utilized in ECDs, electrochromic systems should also undergo simultaneous switching from their saturated color state to a transmissive state (i.e., approach the white point in the CIE color space with a high degree of luminance).¹⁰ Wudl et al. reported on an electrochemically stable neutral-state green conjugated polymer,¹¹ using the donor–acceptor (DA) approach in engineering alternating DA systems exhibiting a two-band absorption in the visible region required for a material to transmit/reflect green and blue-green. Despite their excellent redox stability, the green polymers made were shown to retain a

Received: November 22, 2010

Accepted: February 11, 2011

Published: March 11, 2011

brown hue in their bleached states.^{12,13} Processable green ECPs, that switch to transmissive, have since then been successfully and independently prepared by Reynolds et al.¹⁴ and Toppare et al.^{15,16} Following the first publication of solution-processable green-to-transmissive switching polymers by our group,¹⁴ a series of blue-green and green soluble donor–acceptor conjugated polymers containing 3,4-dioxythiophene (DOT) and 2,1,3-benzothiadiazole (BTD) units were designed, in combination with unsaturated linkages (ethynylene and *trans*-ethylene).¹⁷ This work resulted in a saturated cyan-to-transmissive ECP with fast and highly stable EC performance. In the present study, we demonstrate that this cyan DA polymer composed of the electron-donor 2-ethylhexyloxy-substituted 3,4-propylenedioxythiophene [ProDOT-(CH₂OEtHx)₂] and the electron-acceptor BTD is an excellent EC material for window-type ECDs. In addition, recent developments in our group have provided access to new color hues, including spray-processable blue-to-transmissive,¹⁸ along with red- and orange-to-transmissive switching ECPs.¹⁹ The reason for developing strategies yielding the color black in reflective and window-type ECDs are exemplified by the CMYK four-color system, used in color printing, where K stands for the “key” black color. A combination of cyan, magenta, and yellow inks often gives a brownish hue that is relatively far from the desired rich black color. Furthermore, simultaneous printing of CMY inks often leads to an excess of material, leading to soaking of the paper substrate, or spreading over plastic substrates, which results in “ink-bleeding” defects.²⁰ When considering residential/office smart window and display applications, physiological and psychological components of the color perception should be taken into account. For example, neutral achromatic colors provide an unmitigated view of the environment without altering the original colors; their low brightness minimizes eye fatigue and develops a calm, non-distractive atmosphere.

A growing demand for various non-emissive display applications including e-paper/e-book devices, signage, and EC tags/labels has motivated studies of achromatic black-to-colorless switching electrochromes, such as metal oxides.¹ For example, nanostructured NiO (brown-black to transmissive),²¹ anodically coloring IrO₂ (blue and black to colorless),²² Cu₂O (cathodically coloring black to yellowish),²³ and undoped and N-doped α -WO₃ (transmissive yellow to black and deep blue)²⁴ are possible candidates. While they tend to be robust and stable to heat and light, metal oxides have demonstrated moderate EC performance, including low coloration efficiency (CE) values and relatively slow switching responses (from several tens of seconds to minutes) when compared to surface-bound organic electrochromes. Recently, some metal salts, e.g. almost colorless BiCl₃, that could undergo reversible redox reaction yielding black metallic layers, were utilized in e-paper-type reflective ECDs.²⁵

While organic polymer materials that have uniform broadband absorbance over the entire visible spectrum are especially desirable for photovoltaic^{26–31} and electrochromic applications, the synthesis of a black-to-transmissive switching conjugated ECP remained a challenge for many years. For instance, poly-2-(2-thienyl)-1H-pyrrole was shown to switch from brown-orange to black³² and a phosphole-EDOT copolymer was reported to display blue-to-black EC behavior.³³ Our group has reported on two methods to prepare soluble and spray-processable black-to-transmissive switching polymer electrochromes.^{34,35} The corresponding black polymer (ECP-B)³⁴ demonstrates a set of

properties that makes it promising electrochromic material including high EC contrast (relative luminance change of ~50%), fast color change from black to a transmissive pale blue, along with excellent long-term ambient stability (over 10 000 cycles). To the best of our knowledge, this is the most stable (cycle life), fast switching black-to-transmissive electrochrome with the highest coloration efficiency (>300 cm²/C) among inorganic and organic electrochromic materials reported to date. Large-scale batches of the black-to-transmissive ECP prepared via our first method,³⁴ having essentially the same chemical structure, were found to exhibit a more distinct dark purple-blue tone, which will be designated as “ink-black” (ECP-i-B) in this manuscript.

In addition, black-to-clear redox switches can be attained by mixing two or three ECPs together. With this purpose, Sonmez et al. have reported on a face-to-face combination of RGB polymers on indium tin oxide (ITO)/glass slides in liquid electrolyte and in dual-polymer ECDs exhibiting various intermediate color tones obtained from color mixing.^{12,36} Subsequently, we have demonstrated a pseudo-three-electrode device (P3-ECD) composed of two ECPs of complementary neutral-state color (purple-to-transmissive and green-to-transmissive) in conjunction with a minimal-color-changing polymer (MCCP, specifically PProDOP-N-EtCN).³⁷ The utilization of dual-polymer electrochromic film characterization under bipotentiostatic control³⁸ in the P3-ECD enabled access to an attractive palette of colors, including deep blue-black, and a transmissive state.

In this contribution, we report on the construction and characterization of black-to-transmissive window-type ECDs, using individual and multiple polymer electrochromic materials, in conjunction with an electroactive non-color-changing counter electrode polymer layer (NCCP). As the NCCP, we utilize an organic nitroxide radical polymer: poly(2,2,6,6-tetramethylpiperidinyloxy-4-yl methacrylate) (PTMA). PTMA is highly transparent and colorless in the visible region, exhibits rapid electron transport, and has potentially useful ECD performance, as already demonstrated by Nishide et al. and by Vasilyeva et al.^{39,40} In comparison with complementary anodically/cathodically coloring electrochromic polymer combinations, the EC/NCCP polymer combination leads to a larger EC contrast, retains color purity of the EC system, and induces higher transmittance of devices in the bleached states.^{40,41} Films essentially black in color were spray-processed from solutions of the polymers in various combinations as follows: (1) individual black polymer (ECP-B); (2) individual “ink-black” polymer (ECP-i-B, analogous to ECP-B, but produced on a larger scale, and has more “dark purple-blue” neutral-state color; see Section 3.1); (3) solution blends of magenta (ECP-M) and cyan (ECP-C) polymers; and (4) ECP-M spray-cast over an ECP-C layer to approach a dark ink-black color in window ECDs.

2. EXPERIMENTAL SECTION

2.1. Materials. Lithium tetrafluoroborate (LiBF₄, anhydrous, 99.998%), poly(methyl methacrylate) (PMMA, $M_w = 996\,000$ g mol⁻¹), ferrocene (Fc), toluene, and ethylene carbonate (Ec) were purchased from Aldrich and used as received. The electrolyte salts and ionic liquid 1-ethyl-3-methylimidazolium bis-(trifluoromethylsulfonyl)imide (EMI-BTI, electrochemical grade, >99.5%, Covalent Associates, Inc.) were stored in an argon-filled drybox. Propylene carbonate (PC), dichloromethane (DCM), and acetonitrile (ACN), purchased from

Sigma–Aldrich, were distilled and dried before use. Glass beads (100 μm) were obtained from BioSpec Products, Inc., washed with acetone, and dried in air. ECP-M,⁴¹ ECP-C,¹⁷ and ECP-B³⁴ were synthesized according to the methodologies previously reported. The NCCP poly(2,2,6,6-tetramethylpiperidinyloxy-4-yl methacrylate) (PTMA) and “ink-black” polymer (ECP-i-B) were provided by BASF. For the experimental details for the synthesis of ECP-i-B (analogous to ECP-B, but produced on a substantially larger scale, see Section 3.1 and the Supporting Information). The polymer films were spray-cast onto electrode plates using an airbrush (Iwata-eclipse HP-BS) at an argon pressure of 15–20 psi. ECP-M and ECP-B were sprayed from 2 mg/mL solutions in toluene; ECP-C was processed from a 0.3 mg/mL solution in toluene, because of its relatively low solubility; ECP-i-B was spray-cast from a 2 mg/mL solution in DCM. The ECP-C/ECP-M solution blend was prepared in chloroform, because of the limited solubility of the cyan polymer in toluene. NCCP films were spray-cast as a 1:4 (weight ratio) of a PTMA/PMMA mixture in toluene (15 mg PTMA/60 mg PMMA/60 mL toluene solution) and dried for 40 min at 80 °C in a vacuum oven before characterization. All polymer solutions were filtered through 0.45 μm Whatman Teflon (PTFE) syringe filters prior to spraying. ITO-coated polished float-glass slides CG-51IN-CUV (7 mm \times 50 mm \times 0.7 mm, $R_s = 8\text{--}12 \Omega/\square$) and CG-51IN-S107 (25 mm \times 75 mm \times 0.7 mm, $R_s = 8\text{--}12 \Omega/\square$) were obtained from Delta Technologies, Ltd. [Note: R_s denotes surface resistivity.] Contacts for the electrodes were made from conductive adhesive copper tape (1131, 3M).

2.2. Materials Characterization. The thickness of the EC films was controlled by monitoring optical density values at the λ_{max} of each polymer film while spraying, using a Genesys 20 Spectrophotometer (Thermo Electron Corporation). The surface morphology of the spray-cast polymer films was studied using a Leica DM 2500 P polarized optical microscope (McBain Instruments) with a Leica DFC 295 3MP digital color camera (standard resolution of 2048 \times 1536 megapixels). All micrographs were collected at a 10 \times magnification, with an exposure of 3.6 ms and a saturation of 0.9, and images were not altered and represent true colors of the polymers (color is monitored vs a white point on the color diagram built in the Leica Application Suite V3.3.0 software). Electrochemical studies of the polymer films were carried out in a single-compartment three-electrode cell with a Pt flag as the counter electrode, a Ag/Ag⁺ reference electrode calibrated using a 5 mM Fc/Fc⁺ in 0.1 M LiBF₄/PC electrolyte solution, and ITO-coated glass slides as working electrodes, using an EG&G Model PAR 273A potentiostat/galvanostat. The differential pulse voltammetry (DPV) experiments used a step size of 2 mV, a step time of 0.035 s, and amplitude of 100 mV. Spectroelectrochemistry and chronoabsorptometry/chronocoulometry experiments were carried out on a Varian Cary 500 Scan UV–vis–NIR spectrophotometer. Colorimetry measurements performed with the use of a Minolta CS-100 Chroma Meter. The samples were illuminated from behind with a Graphilite D5000 GLX Transparency Viewer with a built-in LiteGuard quality control monitor (GTI Graphic Technology, Inc.) in a light booth designed to exclude external light. The conductivity of the gel electrolyte was measured using a Fisher Scientific Accumet AB30 conductivity meter with a four-cell conductivity probe (cell constant = 1.0 cm^{-1}) calibrated with traceable conductivity standard solutions. Photographs of the polymer solutions and films were made in a light booth; photographs of devices were made either in a light booth

(transmissive mode) or on the bench (reflective mode), using a digital camera (FinePix S7000, Fuji Photo Film Co., Ltd., Japan, with a close-up photography option). All photographs are presented as received without altering the color brightness or saturation parameters.

2.3. Assembly of Dual-Polymer Window-Type ECDs. Two ITO/glass electrodes were spray-coated with an electrochromic polymer film and NCCP polymer blends (with an active device area of 2.4 cm^2) of controlled thicknesses. EC polymer films for the working electrodes were sprayed using the following individual and multi-polymer materials: (1) individual polymer solutions (ECP-M, ECP-C, ECP-B, and ECP-i-B polymers), (2) blended solution of ECP-C and ECP-M (1:1 weight ratio in DCM), and (3) an ECP-M polymer layer sprayed on top of an ECP-C polymer layer. The ECP films were then oxidatively doped while the counter electrode with NCCP was neutralized in a 0.1 M LiBF₄/PC electrolyte solution prior to device assembly to ensure balance of the charge. The highly transparent and conducting (6.5 mS cm^{-1}) gel electrolyte was composed of 7.2% EMI-BTI, 7.0% of PMMA, 48.1% PC, 37.7% Ec (wt %), and 5 mg of glass beads (100 μm) per 12 mL of solvent, with the latter being used to maintain a fixed gel electrolyte layer thickness when the device was assembled. The gel was prepared by adding PMMA and glass beads to a hot (60 °C) mixture of solvents (PC, Ec) and EMI-BTI with subsequent stirring of the resulting electrolyte overnight. Device construction and testing was carried out under ambient conditions. Devices were encapsulated using extra fast (1–3 min) curable epoxy (Hardman double-bubble epoxy #4001). Blank devices consisting of two facing ITO slides with gel electrolyte sandwiched between them, without the electroactive polymer layers, were prepared for all background optical measurements. The demonstration “butterfly” device (1.7 in. \times 2.7 in. in size) was constructed on In₂O₃/Ag/Au coated PET substrates (surface resistivity of $\leq 10 \Omega/\square$, Aldrich), using a 2.5 mS cm^{-1} gel electrolyte composed of 0.1 M LiClO₄, 8.0 wt % of PMMA, and 10 mg of glass beads per 10 mL of PC:Ec (1:1). Spraying a magenta layer over the cyan, an “ink-black” color has been achieved; the NCCP was utilized as the counter electrode material.

3. RESULTS AND DISCUSSION

3.1. Materials Approach to Attain Black-to-Transmissive EC Change. In this work, both individual black polymers (ECP-B and its structural analog, ECP-i-B) and mixed multi-polymer materials (solution blends and bilayers comprised of the ECP-M and ECP-C polymers) were used to achieve black-to-transmissive color-changing ECDs. The repeat unit structures of the polymers are presented in Figure 1.

ECP-B was synthesized by copolymerizing a symmetrical DAD monomer consisting of electron-donating ProDOT-(CH₂OEtHx)₂ flanking electron-accepting BTD units (corresponding to the monomer repeat unit of ECP-C; see Figure 1) with free ProDOT-(CH₂OEtHx)₂ monomer (corresponding to the monomer repeat unit of ECP-M; see Figure 1) in a random fashion but in appropriate molar feed ratio. Details concerning the experimental conditions employed in the synthesis of the above-mentioned monomers and ECP-B can be found in previously reported work from our group³⁴ (see Table S1 in the Supporting Information for the ECP-B characterization data). As shown in Figure 2, ECP-B exhibits a broad absorption, spanning the visible spectrum from 400 nm to 750 nm, resulting in a particularly dark blue-black color in its neutral state, and

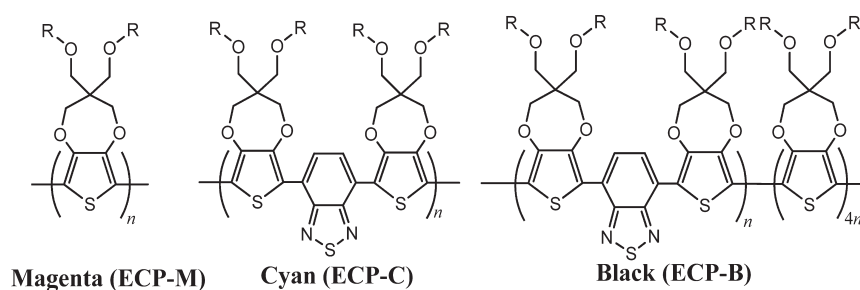


Figure 1. Repeat unit structures of the magenta (ECP-M), cyan (ECP-C), and black (ECP-B) polymers, where R = 2-ethylhexyl. [ECP-i-B is structurally analogous to ECP-B, but was produced on a substantially larger scale. Its neutral state color is “dark purple-blue”, as a result of the longer ProDOT segments embedded in the copolymer.]

bleaches upon oxidation to a transmissive pale blue tint. ECP-i-B was synthesized on a substantially larger scale and using experimental conditions almost identical to those used for the laboratory-scale synthesis of ECP-B (see the Supporting Information). Nevertheless, the molecular composition of the ECP-i-B, as a structural analogue of the ECP-B, was confirmed by elemental analysis (see Table S1 in the Supporting Information).

The redox properties of the ECP-B and ECP-i-B were compared via cyclic voltammetry (CV) and differential pulse voltammetry (DPV). The polymer films were spray-cast onto ITO-coated glass slides and redox-cycled at a 50 mV s^{-1} scan rate between -0.2 V and $+0.7 \text{ V}$ in a $0.1 \text{ M LiBF}_4/\text{PC}$ electrolyte solution until they reached a stable and reproducible electrochemical response. A platinum flag was used as the counter electrode and Ag/Ag^+ as the reference electrode, which was subsequently calibrated to the Fc/Fc^+ redox couple. Both polymer films were stable during the cycling, retaining 95% of their peak anodic and cathodic currents after 200 switches. The CVs of the ECP-B and ECP-i-B display similar redox behavior with slightly lower oxidation onset (within tens of millivolts) for the ECP-i-B in comparison with those of the ECP-B (see Supporting information, Figure S1 and Table S2). The lower oxidation peak and oxidation onset values, as well as a more reversible oxidation process in the case of the ECP-i-B in comparison with ECP-B are likely due to a higher content of relatively long segments composed of the electron-rich ProDOT unit incorporated in the main-chain of the ECP-i-B.

Figure 2 overlays the optical absorbance spectra of the ECP-B and ECP-i-B films spray-cast onto ITO-coated glass and switched in $0.1 \text{ M LiBF}_4/\text{PC}$ electrolyte solution between their extreme states from -0.2 V to 0.65 V vs. Ag/Ag^+ reference electrode. More pronounced peak absorptions at 550 and 592 nm and a more saturated deep purple-blue color are observed in the case of the ECP-i-B, because of longer PProDOT blocks. Note that the ECP-i-B, relative to the ECP-B, undergoes more-effective bleaching upon oxidation, effectively depressing the residual absorbance at ca. 700 nm (where the two neutral films were cast to have identical absorbances), thus resulting in a doped state of somewhat higher transmittance. This last observation is also consistent with the higher content of significantly longer ProDOT segments in the corresponding copolymer.

To obtain a multitude of color hues including the color black, it is theoretically possible to combine polymers exhibiting subtractive primary colors (CMY). At the same time, mixing saturated magenta and cyan ECPs should allow “mimicking” of the dark “ink-black” color as a possible alternative to the use of the ECP-i-B copolymer. ECP-C/ECP-M color mixing was produced in two different ways in this work: (1) blending

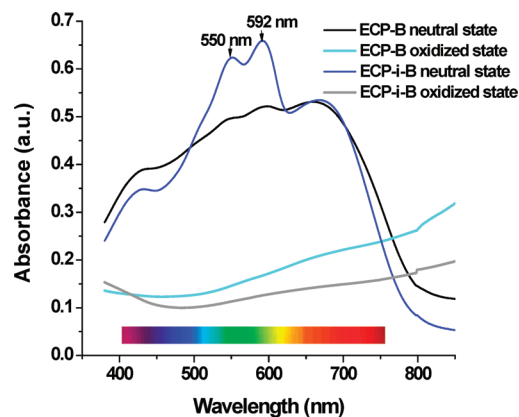


Figure 2. Optical absorbance spectra of the ECP-B and ECP-i-B (the structural analog of the ECP-B, having a more “dark purple-blue” neutral-state color) films spray-cast onto ITO-coated glass slides in their extreme absorbing and transmitting states. The polymers were electrochemically switched in a $0.1 \text{ M LiBF}_4/\text{PC}$ electrolyte solution between their colored (-0.2 V) and bleached states (0.65 V) vs. Ag/Ag^+ reference electrode.

ECP-C and ECP-M polymer solutions in appropriate ratios with subsequent spray-casting of the blended solution, and (2) spraying an ECP-M layer on top of an ECP-C layer (the ECP-C/ECP-M bilayer in the text).

Solution optical absorbance spectra of the ECP-M, ECP-C, ECP-i-B, ECP-B polymers, and ECP-C/ECP-M (1:1 weight ratio) polymer blend in chloroform are shown in Figure 3a. ECP-M exhibits a vibrant magenta color with the interband $\pi-\pi^*$ transition split into a shoulder at $\sim 505 \text{ nm}$ and two distinct peaks at 540 and 573 nm, attributed to vibronic coupling.^{42–44} ECP-C possesses a dual band of absorption in the visible spectrum consisting of short- (396 nm) and long-wavelength (642 nm) bands, which we attribute to the electron-rich portion of the alternating polymer backbone and to the intramolecular donor–acceptor interaction arising from the covalent bonding of electron-rich (ProDOT) and electron-deficient (BTD) building units, respectively.³⁴ Between these two absorption bands, a gap of transmission in the blue-green region is evident with a minimum of absorption positioned at $\sim 450 \text{ nm}$, giving this polymer a saturated cyan neutral-state color. A relatively reduced solubility of ECP-C, compared to ECP-M, ECP-i-B, and ECP-B in toluene (common casting solvent), justified the use of chloroform, where all polymers were found to dissolve instantaneously at room temperature.

With careful comparison of the solution absorbance spectra of the ECP-C/ECP-M blend, as well as the ECP-i-B and ECP-B

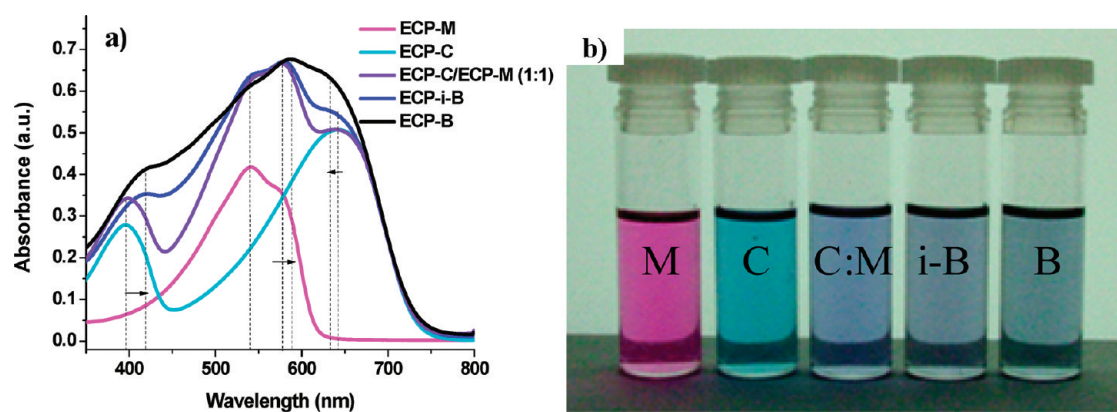


Figure 3. (a) Solution optical absorbance spectra of ECP-M, ECP-C, ECP-C/ECP-M solution blend, ECP-i-B (analogous to ECP-B, but produced on a larger scale, and inherently more “dark purple-blue”), and ECP-B in chloroform. [Concentrations of the polymer solutions: (1) $C_{\text{ECP-M, ECP-C, ECP-C/ECP-M}} = 0.02$ mg/mL and (2) $C_{\text{ECP-i-B, ECP-B}} = 0.064$ mg/mL.] (b) Photograph of the polymer solutions with the specified concentrations in chloroform is made in a light booth.

polymers, several differences can be appreciated. For example, the presence of transmission windows with absorption minima located at ca. 440 and 620 nm between the high- and low-energy transitions in the spectra of the ECP-i-B contrasts with the more homogeneously filled spectral absorption of ECP-B between its respective absorption maxima. The progressive filling of this transmission window is even more obvious when successively comparing ECP-C to the ECP-C/ECP-M blend, to ECP-i-B, and finally to ECP-B. As a result, a gradual color change from a distinct saturated blue-purple color for the ECP-C/ECP-M blend, to an “ink-black” color for the ECP-i-B, and to an almost-achromatic black for the ECP-B (see photographs of polymer solutions in Figure 3b) is observed. As previously introduced in our work, an additional “merging” effect between the short- and long-wavelength absorption peaks is also detected here. This effect can be modulated by varying the relative content of electron-rich ProDOT and electron-deficient BTD heterocycles in DA polymers.³⁴

To attain a neutral-state “ink-black” color without employing ECP-i-B, the magenta polymer was spray-cast on top of the cyan polymer, hence forming an ECP-C/ECP-M bilayer film. Figure 4 compares the solid-state optical absorbance spectra of ECP-M, ECP-C, the ECP-C/ECP-M bilayer, and ECP-i-B polymer films in their neutral states. Prior to the spectral measurements, the polymers were electrochemically cycled between -0.2 V to 0.7 V vs. Ag/Ag^+ reference electrode in a 0.1 M LiBF_4/PC electrolyte solution ~ 20 times until stable voltammograms were recorded. Subsequently, the polymers were neutralized at -0.2 V and the absorbance spectra of their colored states were measured, which revealed a similar trend to those taken in solution. In the case of the ECP-C/ECP-M bilayer film, where a simple physical overlay of cyan and magenta polymers was achieved, the optical transition bands are more distinct and separated with open transmission gaps in the blue (~ 460 nm) and in the red (~ 630 nm) portions of the spectrum, resulting in a highly saturated purple-blue color. In contrast, the broader absorbance spectrum of the ECP-i-B polymer with “merged” short- and long-wavelength transitions induces a much more pronounced “ink-black” color. The bathochromic shift of all of the optical transitions, relative to the solution spectra, is expected as we examine the polymer films due to a higher degree of order and coplanarity of the polymer chains in the solid state.

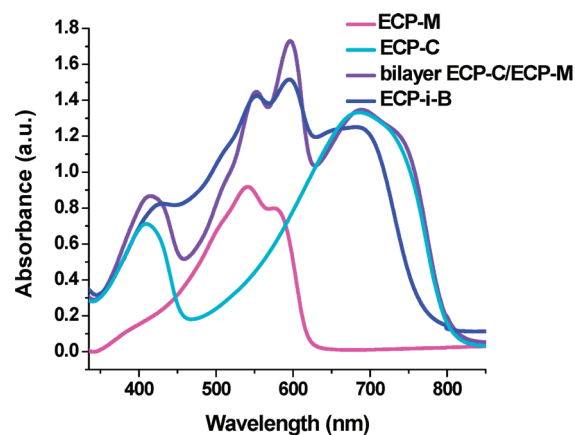


Figure 4. Optical absorbance spectra of the ECP-M, ECP-C, ECP-i-B (analogous to ECP-B, but produced on a substantially larger scale, and inherently more “dark purple-blue”), and ECP-C/ECP-M bilayer polymer films in their colored states. Polymers were spray-cast onto ITO-coated glass slides, electrochemically switched (~ 20 cycles) from -0.2 V to 0.7 V vs. Ag/Ag^+ reference electrode in a 0.1 M LiBF_4/PC electrolyte solution, and then neutralized (at -0.2 V).

It is well-known that varying the electrochromic polymer processing conditions, such as spray-casting or spin-casting from different solvents, can induce drastic changes in polymer surface morphology and, thus, modify the performance properties of the resulting films.⁴⁵ A set of organic solvents (toluene, DCM, chloroform, chlorobenzene, and their mixtures at various ratios) was used in this work to obtain the most compact and homogeneous polymer layers. The minimal level of polymer aggregation in an optimal processing solution reduces light scattering of the resulting polymer films in their neutral and oxidized states, introducing a high transmittance to the oxidized form and an enhanced EC contrast. Figure 5 shows optical micrographs of the ECP-M, ECP-C, ECP-C/ECP-M solution blend, ECP-C/ECP-M bilayer, ECP-i-B, and ECP-B polymer films of almost-equal absorbance ($A \approx 1.0$ au at the maximum wavelength (λ_{max}) of the polymer), spray-cast onto ITO-coated glass slides. The micrographs, which were collected at a $10\times$ magnification, 3.6 ms exposure, and 0.9 saturation, illustrate reliable colors for the studied polymer materials. The colors were monitored vs. a white

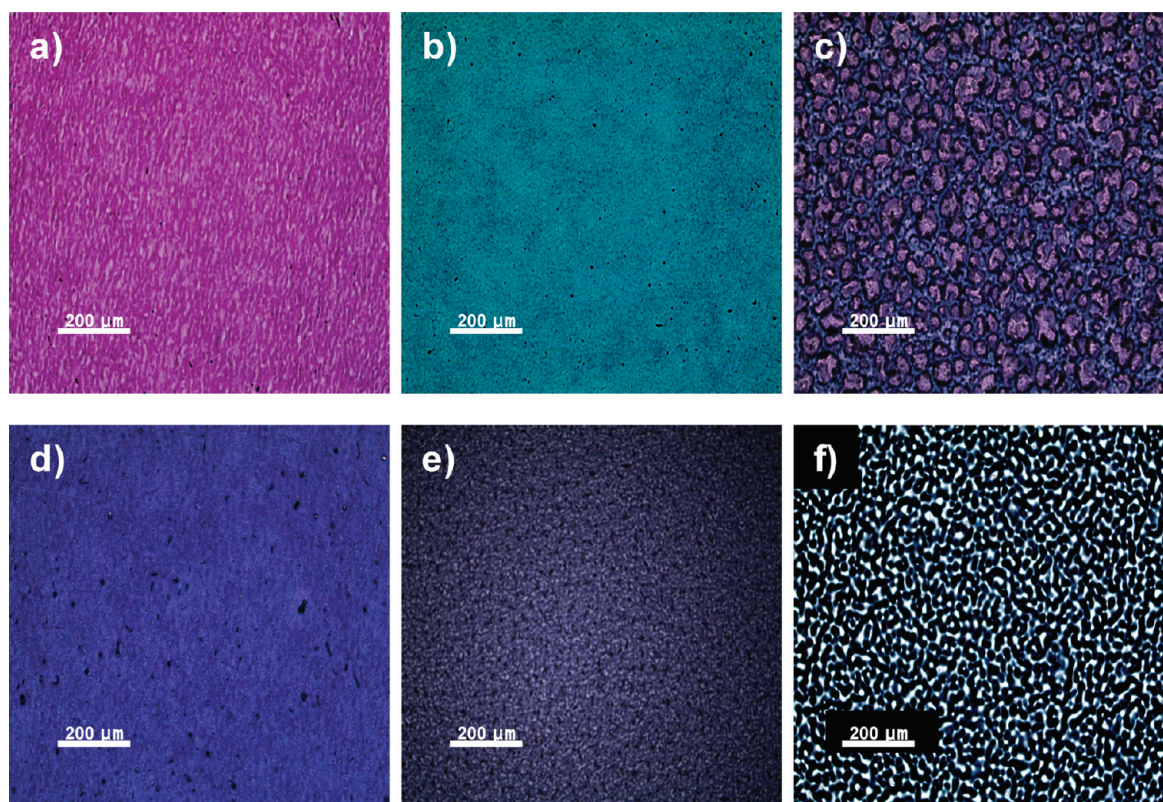


Figure 5. Micrographs of the polymer films spray-cast onto ITO-coated glass slides: (a) ECP-M, (b) ECP-C, (c) ECP-C/ECP-M solution blend, (d) ECP-C/ECP-M bilayer, (e) ECP-i-B (analogous to ECP-B, but produced on a substantially larger scale, and inherently more “dark purple-blue”), and (f) ECP-B polymer films. All micrographs were measured at a 10 \times magnification.

point on the color diagram as a reference, using a “check color” option in the Leica Application Suite V3.3.0 software. Toluene, chloroform, DCM, and their mixtures were used as processing solvents to deposit polymer films with an optimized morphology. After several trial experiments, toluene was chosen as the solvent for processing ECP-M, ECP-C, ECP-C/ECP-M bilayer and ECP-B polymers. The ECP-C/ECP-M blend was dissolved in chloroform, because of the relatively low solubility of the ECP-C component in other solvents and difficulty in maintaining the necessary ECP-C:ECP-M ratio needed to obtain the “ink-black” color. ECP-i-B, sprayed from DCM, gave the smoothest compact film (Figure 5e), whereas the micrographs of the ECP-B show a coarser morphology (Figure 5f). In contrast to all of the other polymer films, the ECP-C/ECP-M solution blend produced the coarsest films, exhibiting a distinct phase separation (Figure 5c), which is not surprising for a polymer blend. The film is composed of purple-magenta domains of a large size distribution (from 10 μm to 100 μm) embedded in a cyan-colored background layer. The presence of these large aggregates resulted in non-uniform translucent films that are not suitable for implementation in window ECDs. Further careful optimization of the processing solvent system will be required for the multi-material EC polymer blend solutions to be successfully employed to produce compact transparent films.

3.2. Dual Polymer Black-to-Transmissive ECDs. Dual polymer black-to-transmissive window ECDs on ITO/glass were assembled as illustrated in Figure 6. The electrochromic polymer film was composed of either individual ECP-B and ECP-i-B polymers, or an ECP-C/ECP-M polymer bilayer to approach an “ink-black” color state. The ECP films were used in conjunction

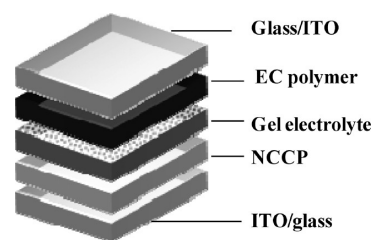


Figure 6. Schematic diagram of the dual polymer black-to-transmissive ECD configuration.

with a colorless NCCP counter electrode layer, as well as with a highly conducting (6.5 mS cm^{-1}) transparent gel electrolyte sandwiched between two electrodes. The absorbance of the ECP-B and ECP-i-B polymer materials was maintained at $A \approx 0.6$ au (thinner layer) or at $A \approx 1.35$ au (thicker layer) at λ_{max} (665 nm), and the absorbance of the ECP-M and ECP-C films also at λ_{max} (540 and 685 nm, correspondingly). Redox charges of the ECP and NCCP films were matched prior to device fabrication, as probed by stepping the potential between -0.2 V and $+0.75$ V in a 0.1 M LiBF_4/PC solution, to provide a balanced number of redox sites in both polymers. The ECP films were oxidized, while the film of NCCP was neutralized potentiostatically prior to device construction.

Prior to quantitative measurements on the ECP-C/ECP-M bilayer-based devices, and to provide a more aesthetic visual representation and demonstration of the cyan and magenta ECP bilayer producing an ink-black color in window devices, a multi-colored “butterfly” ECD was designed and assembled (see

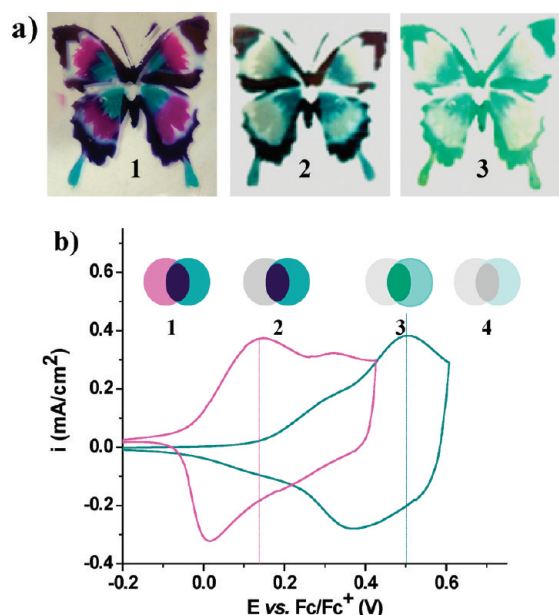


Figure 7. (a) Photographs of a multicolored window ECD on $\text{In}_2\text{O}_3/\text{Ag}/\text{Au}$ -coated PET electrodes (with an active area size of 2.7 in. \times 1.7 in.), using ECP-M and ECP-C spray-cast onto the electrode through a “butterfly”-shaped mask. The “black” part of the device is composed of the ECP-C/ECP-M bilayer (the magenta layer was sprayed on top of cyan layer). The ECD was switched from neutral (1) to intermediate oxidized states (2 and 3). (b) Cyclic voltammograms of the individual ECP-M and ECP-C; inset shows a gradual color change during the oxidation process in the device from neutral (1) to the completely bleached (4) state (which is not attained, because of the electrode material (ITO) breakdown).

Figure 7). This ECD (with an active area size of 2.7 in. \times 1.7 in.) was fabricated using two facing transparent flexible electrodes ($\text{In}_2\text{O}_3/\text{Ag}/\text{Au}$ -coated PET) separated by a thin layer of gel electrolyte, to allow color switching. ECP-M and ECP-C were spray-cast onto the electrodes through several shadow masks. The NCCP was used as the counter electrode material. Photographs of the active area of the “butterfly” ECD in its colored (neutral) and two oxidized states were taken in a light booth at -0.5 , 1.5 , and 2.8 V, respectively (see Figure 7a). Photographs were taken at slightly different angles, which resulted in minor changes in the lighting and background colors. Figure 7b shows the cyclic voltammograms of the ECP-M and ECP-C, and the insets illustrate the colored and oxidized states of the butterfly ECD. The ECP-M and ECP-C layers present in the butterfly ECD demonstrate bright magenta and cyan colors; the places where the magenta and cyan layers overlap have ink-black color (neutral state 1). Because of a significant difference in oxidation potentials of the ECP-M and ECP-C polymers ($E_{\text{pa,ECP-M}} = 0.14$ V and $E_{\text{pa,ECP-C}} = 0.50$ V vs. Fc/Fc^+), the magenta layer bleaches first (state 2) where the ECP-C/ECP-M bilayer retains its “ink-black” color, since a thicker bilayer film has a higher resistance, compared to the ECP-M layer, and requires higher oxidation potentials to start changing the color. A further increase of the oxidation potential (state 3) results in a bleaching of the cyan polymer layer and an incomplete color change of the ECP-C/ECP-M bilayer from “ink-black” to green-blue. A higher degree of oxidation must be applied to bleach the cyan and the ECP-C/ECP-M bilayer completely (state 4, which is not attained because of electrode material breakdown). Unfortunately, our attempt to operate the device

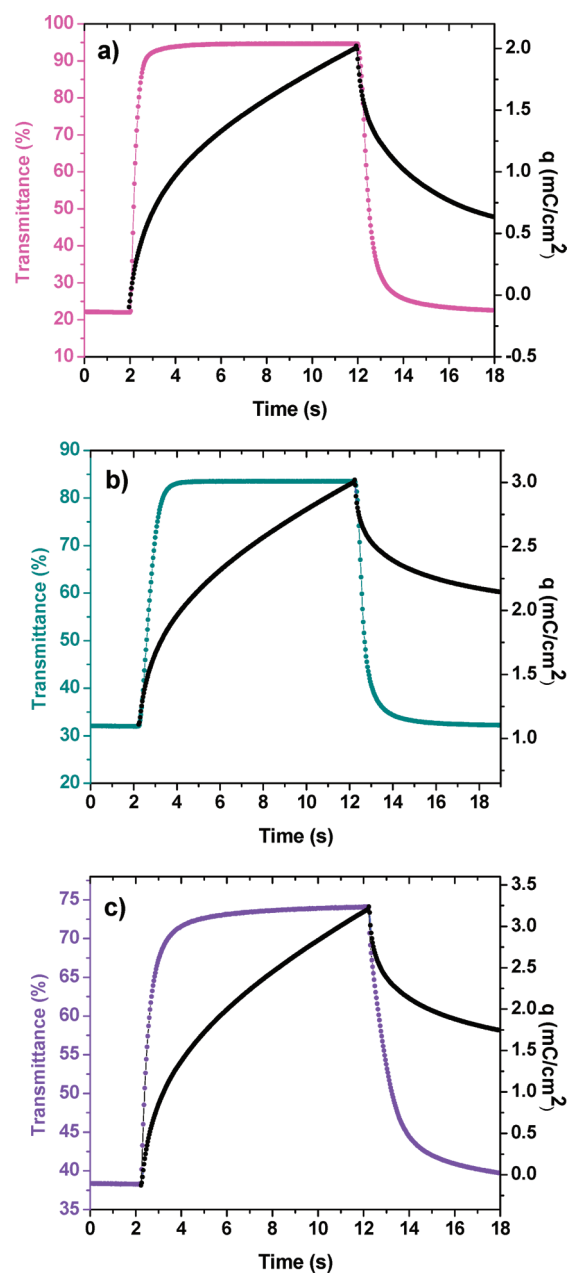


Figure 8. Tandem chronoabsorptometry and chronocoulometry experiments for window ECDs: (a) ECP-M ECD (stepped from -0.2 V to $+2.2$ V in 10 s intervals at 596 nm); (b) ECP-C ECD (stepped from 0.0 V to $+2.2$ V in 10-s intervals at 682 nm); (c) ECP-C/ECP-M bilayer ECD (stepped from -0.2 V to $+2.4$ V in 10 s intervals at 550 nm).

while applying mechanical bending motions failed, because of the inherent fragility of the indium oxide conducting electrode coating, resulting in discontinuance of the ECD switching to the fully bleached state (fully oxidized state 4 in Figure 7b). This further reinforces the need to develop and apply electrode materials tolerant to mechanical constraints, such as flexible single-walled carbon nanotube films.

A tandem chronoabsorptometry/chronocoulometry measurement was used to evaluate the switching times and the composite coloration efficiency (CCE)⁴⁶ at 95% of the total optical change of the ECP-M, ECP-C, and ECP-C/ECP-M bilayer window devices (see Figure 8 and Table 1). The ECDs were switched

Table 1. Optical, Switching Time, and Coloration Efficiency Characteristics of the ECP-C, ECP-M, and ECP-C/ECP-M Bilayer Window Devices, Using Non-Color-Changing Counter Electrode Polymer (NCCP) Counter Electrode Material

ECD system: ECP vs NCCP	%T ^a	$\Delta\%T^a$	%Y ^a	ΔY	Colored State			Bleached State			time ^a (s)	CCE ^a (cm ² /C)
					L*	a*	b*	L*	a*	b*		
ECP-M ($A \approx 0.6$)	89	67	90	52	60	26	-25	97	-1	1	0.6	1017
ECP-C ($A \approx 0.6$)	80	48	89	35	76	-18	-14	96	1	-1	1.0	570
ECP-C/ECP-M bilayer ($A \approx 0.6$)	71	33	80	36	68	1	-21	92	-2	0	1.6	188
ECP-C/ECP-M bilayer ($A \approx 1.3$)	52.5	41	63	56	32	13	-46	83	-3	-6	7.5	126

^a %T and %Y values are given for the bleached state. Switching %T parameters are reported for 95% of the full optical switch between the colored and bleached states.

between their colored and bleached states by stepping the applied voltage (a potential difference of $\Delta E = 2.2-2.6$ V) in intervals of 10 s. The %T was monitored at an optimal single wavelength (λ_{\max}), giving the highest transmittance contrast at 596, 682, and 550 nm for the ECP-C, ECP-M, and ECP-C/ECP-M-based devices, respectively. The percent relative luminance (%Y) values of the devices were measured colorimetrically as a function of potential, using the CIE 1931 Yxy color space.¹⁰ Colorimetry is an effective tool providing accurate information on the precise color characteristics and a “real” transmissivity of the ECDs as they appear to the eye of a standard human observer. The color of the window ECDs is characterized quantitatively, utilizing the CIE 1976 $L^*a^*b^*$ system, where L^* represents lightness (ranging from 0 to 100), and a^* and b^* are hue and chroma values, respectively.⁴⁷ Positive and negative a^* values correspond to red and green hues, respectively, while positive and negative b^* values denote yellow and blue chromas.

The ECP-M polymer is as an excellent electrochromic material, since its high optical contrast ($\Delta OD = \log \%T_{0.95\text{bleached}}/\%T_{\text{colored}}$) occurs with a minimal amount of charge injection/ejection. As illustrated by Figure 8a, the magenta ECD exhibits a large optical modulation (67%T) achieved rapidly (within 0.6 s) leading to a high CCE (>1000 cm²/C). The ECP-M device shows a saturated magenta color with almost equal values of the red hue ($a^* = 26$) and blue chroma ($b^* = -25$) in its neutral state, changing to a particularly transparent, almost colorless bleached state upon electrochemical oxidation (a high lightness parameter ($L^* = 97$) with minimal $a^* = -1$ and $b^* = 1$ values). These results obtained are in a good agreement with those reported on ECP-M/NCCP ECDs, using a LiClO₄/PMMA/PC:Ec gel electrolyte.⁴⁰

When compared with ECP-M, the ECP-C polymer exhibits a higher oxidation potential and a lower switching speed in the electrolyte system employed (switching times of 0.4 and 0.9 s, respectively, for ECP-M and ECP-C films of comparable optical densities). Nevertheless, ECP-C exhibits a saturated cyan color and excellent electrochemical stability (10 000 double step cycles with a minimal EC contrast loss).¹⁷ The slower charge transport in the case of the ECP-C resulted in a slower (1.0 s) switching and less-efficient color change (CCE = 570 cm²/C) for the cyan-to-transmissive ECDs (with slightly higher contribution of a green hue, $a^* = -18$, than that of a blue chroma, $b^* = -14$) (see Figure 8b). Overall, both the magenta and cyan window devices demonstrated a useful electrochemical stability upon continuous redox switching between their extreme states with a <10% ΔT loss over more than 10 000 cycles. The fact that these devices were fabricated and tested under ambient conditions indicates a high durability of these ECDs.

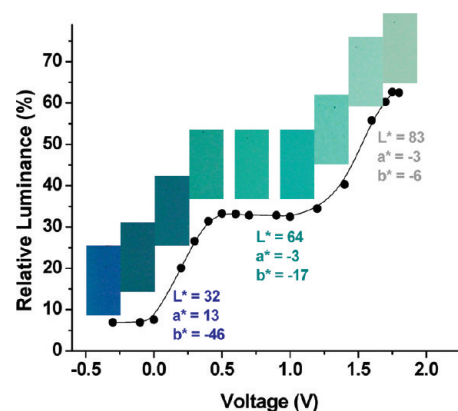


Figure 9. Percent relative luminance (%Y) of the ECP-C/ECP-M bilayer/NCCP window ECD ($A_{\text{ECP-C/ECP-M bilayer}} \approx 1.3$ au), as a function of applied voltage. Actual photographs of the active area of the device (taken in a light booth) at progressively applied voltage illustrate the continuous color change.

Two ECP-C/ECP-M bilayer films of different thicknesses were sprayed onto ITO/glass electrodes for incorporation into ECDs. First, a thinner film (first, the ECP-C layer with $A \approx 0.47$ au at 642 nm was spray-cast onto the substrate, followed by the ECP-M layer being overlaid (sprayed-cast) until the absorbance of the resulting ECP-C/ECP-M bilayer reached $A \approx 0.6$ at 550 nm). Second, a thicker film with $A \approx 1.3$ au was formed in the same manner, with the ECP-C layer having an $A \approx 1.05$ au at 642 nm spray-cast onto the substrate first, followed by the ECP-M layer being overlaid until the absorbance of the resulting ECP-C/ECP-M bilayer reached $A \approx 1.3$ au at 550 nm. In general, the ECP-C/ECP-M bilayer-based devices demonstrate a purple-blue neutral-state color that becomes more absorptive as the film of ECP gets thicker (with less contribution of a red hue, $a^* = 14$, than that of a blue chroma, $b^* = -46$ and a lightness value as low as $L^* = 32$), and that switches to a doped transmissive state, retaining more residual absorption ($L^* = 83$, $a^* = -3$, $b^* = -6$) when the ECP film gets thicker. The ECP-C/ECP-M bilayer ECDs exhibit slower switching speeds (1.6 s for thinner film devices and 7.5 s for thicker film devices) than that observed for the magenta and cyan ECDs (Figure 8c). Since the charge density required for the coloration/bleaching of the ECD increases with the polymer film thickness, higher CCE characteristics were obtained for the thinner films. The slower color change, in comparison with the individual ECP-M- and ECP-C-based ECDs, could be due to several reasons, as discussed below.

Figure 9 illustrates the %Y change of the bilayer ECD ($A_{\text{ECP-C/ECP-M bilayer}} \approx 1.3$ au), as a function of applied voltage. Actual photographs of the ECD (taken in a light booth) illustrate a

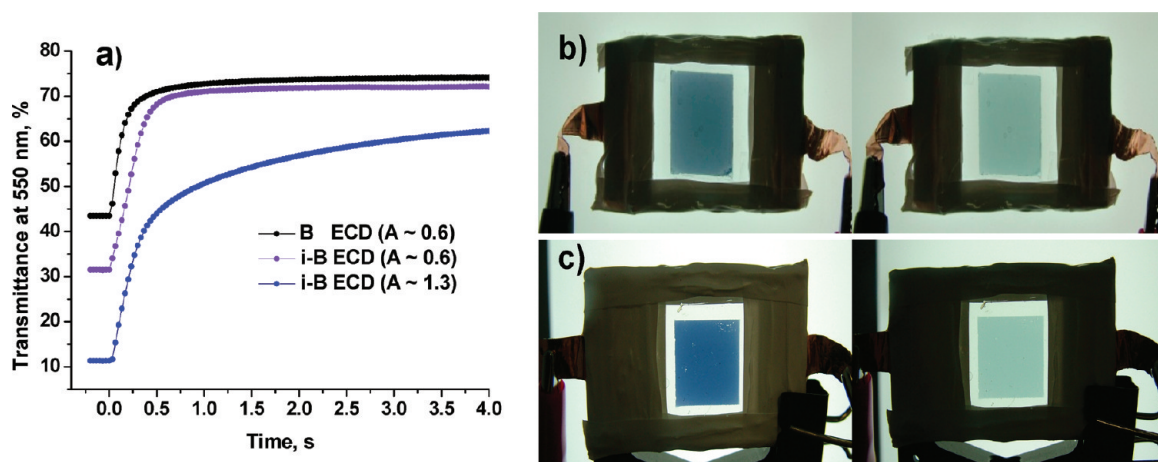


Figure 10. (a) Chronoabsorptometry results for three “black” window devices switched between -0.8 V to $+1.6$ V ($\Delta E = 2.4$ V): (1) ECD with a thin layer ($A = 0.6$) of the ECP-B polymer, (2) ECD with a thin ($A = 0.6$) ECP-i-B polymer, and (3) ECD with a thick ($A = 1.3$) ECP-i-B polymer film. The % T change was measured at $\lambda_{\text{max}} = 550$ nm. Digital photographs of the black-to-transmissive ECDs ((b) ECP-B and (c) ECP-i-B) devices in their colored and bleached states are also shown.

Table 2. Optical, Switching Time, and Coloration Efficiency Characteristics of the ECP-B and ECP-i-B Window Devices, Using NCCP Counter Electrode Material

ECD system: ECP vs NCCP	%T ^a	$\Delta\%T^a$	%Y ^a	$\Delta\%Y$	Colored State			Bleached State			time ^a (s)	CCE ^a (cm ² /C)
					L*	a*	b*	L*	a*	b*		
ECP-B ($A \approx 0.6$)	72	30	77	30.5	76	0	-8	90	-2	-3	0.67	215
ECP-i-B ($A \approx 0.6$)	71	36	80	45.5	65	2	-18	92	-2	-1	0.69	375
ECP-i-B ($A \approx 1.3$)	60.5	50	70	60.5	38	5	-25	87	-3	-2	3.0	238

^a %T and %Y values are given for the bleached state. Switching %T parameters are reported for 95% of the full optical switch between the colored and bleached states.

continuous color change. As clearly seen from Figure 9, because of a significant difference in potentials for electrochemical oxidation in the separate layers of ECP-M and ECP-C, there are two distinct color-transition regions. An initial color change is observed from the “ink-black” to cyan (from -0.2 V to $+0.5$ V), followed by a second color change from cyan to transparent light blue-green (from $+1.0$ to $+2.5$ V), separated by a potential region where almost no color change occurs. Cyclic voltammograms of the ECP-C/ECP-M bilayer film show two oxidation peaks at 0.34 and 0.63 V, presumably characteristic of the ECP-M and ECP-C components of the bilayer (see Figure S1 in the Supporting Information). The origin of the non-color-changing plateau is attributed to a significant difference in oxidation potentials of the ECP-M and ECP-C polymers and, possibly from diffusion limitations in a thick bilayer film (as previously shown in Figure 7b). Another reason for the slow coloration/bleaching of the thick ECP-C/ECP-M bilayer-based ECDs could be the following: a thick ECP multi-polymer film consumes more charge than a thinner one, requiring a balanced amount of charge on the counter electrode. The NCCP counter electrode material consists of a colorless and transparent PTMA/PMMA (1:4 weight ratio) polymer blend annealed at 80 °C. To balance the charge on the working electrode, more blend material is required at the counter electrode. As the thickness of the blend increases, the film becomes more powdery and fragile. It is presumably less conducting, because of partial layer separation from the electrode surface, yielding a morphology that resembles a cracked desert floor (see Figure S2 in the Supporting Information).

Following up on the characterization of the multi-film ECP-C/ECP-M bilayer ECDs, black-to-transmissive window devices were

assembled using the individual ECP-B and ECP-i-B copolymers. As expected, the ECP-B-based devices demonstrate a deeper achromatic black neutral-state color in comparison with the ECP-i-B, as illustrated by the results and photographs in Figure 10. More precisely, as seen in Table 2, the ECP-i-B device exhibits a dark “ink-black” color containing a dominating blue chroma (b^* ranging from -18 to -25 upon going from thin films to thicker films) and a slight red hue contribution. In contrast, the ECP-B-based ECDs (thinner film) did not show any red tone in their neutral state, and they possessed only a moderate blue chroma. Interestingly, the ECP-i-B devices were found to have higher contrasts (16% larger $\Delta\%T$ values) and slightly higher transmittance than the ECP-B-based ECDs at the measured wavelength of 550 nm. In general, the thinner film ECDs switch rapidly with an almost-identical rate (~ 0.7 s), while the thicker-film ECP-i-B-based ECDs modulate color ~ 4 times slower (Figure 10). In general, the all-black ECDs (both individual copolymer- and multi-polymer-based) described in this study demonstrated high EC contrast (up to 50%T and 60%Y) and ΔL^* values (up to 50) comparable to those of the black-to-clear electrochromic polymer window devices previously reported by our group.^{35,37}

It is worth noting that devices using individual ECP-B and ECP-i-B copolymers ($A \approx 0.6$) were found to switch more than twice as fast (< 0.7 s) as those composed of the ECP-C/ECP-M bilayer configuration (1.6 s). In fact, the thicker ECP-i-B-based ECDs demonstrated a faster response (3.0 s), in comparison with the multi-polymer devices (7.5 s). A possible explanation for this result is that, while the individual DA copolymers act as one homogeneous material, the bilayer material has an

inhomogeneous interface between the two polymers, where charge and ion transport can have slower kinetics. The all black ECDs demonstrated a maximum CCE value of 375 cm²/C for the thin-film ECP-i-B-based device, because of a larger optical contrast, in comparison with the ECP-B-based device at its λ_{max} value and a lower charge density in comparison with that required to switch a thicker film. The ECP-B and ECP-i-B thin-film-based ECDs exhibited a transmittance loss of <6.0 after 5000 double potential steps. Thicker ECP-film-based devices demonstrated lower electrochemical stability, presumably because of a partial separation of the thick NCCP layer from the electrode surface.

4. CONCLUSIONS

This paper describes the assembly and characterization of dual polymer black-to-transmissive window-type electrochromic devices (ECDs) on indium tin oxide (ITO)/glass electrodes utilizing an electrochromic π -conjugated polymer (ECP), and a non-color-changing counter electrode polymer (NCCP) as the charge-compensating counter electrode component. The use of the NCCP enhances the EC contrast in the black devices and the color vibrancy in the magenta and cyan control devices.^{40,41} The black color in these window devices was attained using a combination of different material strategies. The individual ECP-B and ECP-i-B (analogous to ECP-B, but produced on a substantially larger scale, and inherently more “dark purple-blue”) copolymers, as well as multipolymer ECP-C/ECP-M bilayer (via color mixing), have been chosen as electroactive electrochromic materials. Although both strategies yielded high contrast ($\sim 50\% \Delta T$) ECDs, devices fabricated with the donor-acceptor (DA) copolymers exhibit a faster bleaching/coloration and more neutral “black” colors than the multi-polymer ECDs. Their solution processability, relatively fast switching (0.7–3.0 s), large contrast (up to 60% relative luminance change), and high transmittance in the bleached states ($\sim 80\%$ relative luminance), along with high stability (thousands of double potential steps) of the ECP-M, ECP-C, ECP-B, and ECP-i-B devices, make them promising materials for various ECD applications, including color-neutral smart windows, non-emissive displays, vision systems, and e-readers.

■ ASSOCIATED CONTENT

S Supporting Information. Experimental details, elemental analysis, electrochemical data, and micrograph of the NCCP film. (PDF) This material is available free of charge via the Internet at <http://pubs.acs.org>.

■ AUTHOR INFORMATION

Corresponding Author

*Phone: 352-392-9151. Fax: 352-392-9741. E-mail: reynolds@chem.ufl.edu.

■ ACKNOWLEDGMENT

We gratefully acknowledge BASF for the funding of this project.

■ REFERENCES

(1) Monk, P. M. S.; Mortimer, R. J.; Rosseinsky, D. R. *Electrochromism and Electrochromic Devices*; Cambridge University Press: New York, 2007.

- (2) Krebs, F. C. *Nat. Mater.* **2008**, *7*, 766–767.
- (3) Ma, C.; Taya, M.; Xu, C. *Polym. Eng. Sci.* **2008**, *48*, 2224–2228.
- (4) Beaupre, S.; Dumas, J.; Leclerc, M. *Chem. Mater.* **2006**, *18*, 4011–4018.
- (5) Invernale, M. A.; Ding, Y.; Sotzing, G. A. *ACS Appl. Mater. Interfaces* **2010**, *2*, 296–300.
- (6) Monk, P. M. S.; Delage, F.; Costa Vieira, S. M. *Electrochim. Acta* **2001**, *46*, 2195–2202.
- (7) Corr, D.; Stobie, N.; Bach, U.; Fay, D.; Kinsella, M.; McAtamney, C.; O'Reilly, F.; Rao, S. N. *Solid State Ionics* **2003**, *165*, 315–321.
- (8) Dyer, A. L.; Reynolds, J. R. In *Handbook of Conducting Polymers: Theory, Synthesis, Properties, and Characterization*; Skotheim, T. A., Reynolds, J. R., Eds.; CRC Press: Boca Raton, FL, 2007; p 20.
- (9) Beaujuge, P. M.; Reynolds, J. R. *Chem. Rev.* **2010**, *110*, 268–320.
- (10) *CIE Technical Report: Colorimetry*, 3rd ed.; Commission Internationale De L'eclairage: Vienna, Austria; 2004.
- (11) Sonmez, G.; Shen, C. K. F.; Rubin, Y.; Wudl, F. *Angew. Chem., Int. Ed.* **2004**, *43*, 1498–1502.
- (12) Sonmez, G. *Chem. Commun.* **2005**, *42*, 5251–5259.
- (13) Sonmez, G.; Sonmez, H. B.; Shen, C. K. F.; Jost, R. W.; Rubin, Y.; Wudl, F. *Macromolecules* **2005**, *38*, 669–675.
- (14) Beaujuge, P. M.; Ellinger, S.; Reynolds, J. R. *Adv. Mater.* **2008**, *20*, 2772–2776.
- (15) Durmus, A.; Gunbas, G. E.; Camurlu, P.; Toppare, L. K. *Chem. Commun.* **2007**, 3246–3248.
- (16) Gunbas, G. E.; Durmus, A.; Toppare, L. K. *Adv. Funct. Mater.* **2008**, *18*, 2026–2030.
- (17) Beaujuge, P. M.; Vasilyeva, S. V.; Ellinger, S.; McCarley, T. D.; Reynolds, J. R. *Macromolecules* **2009**, *42*, 3694–3706.
- (18) Amb, C. M.; Beaujuge, P. M.; Reynolds, J. R. *Adv. Mater.* **2009**, *22*, 724–728.
- (19) Dyer, A. L.; Craig, M. R.; Babiarz, J. E.; Kiyak, K.; Reynolds, J. R. *Macromolecules* **2010**, *43*, 4460–4467.
- (20) McCue, C. *Real World Print Production*; Peachpit: Berkeley, CA; 2007.
- (21) Boschloo, G.; Hagfeldt, A. *J. Phys. Chem. B* **2001**, *105*, 3039–3044.
- (22) Jung, Y.; Lee, J.; Tak, Y. *Electrochem. Solid-State Lett.* **2004**, *7*, H5–H8.
- (23) Neskovska, R.; Ristova, M.; Velevska, J.; Ristov, M. *Thin Solid Films* **2007**, *515*, 4717–4721.
- (24) Nakagawa, K.; Miura, N.; Matsumoto, S.; Nakano, R.; Matsumoto, H. *Jpn. J. Appl. Phys.* **2008**, *47*, 7230–7235.
- (25) Imamura, A.; Kimura, M.; Kon, T.; Sunohara, S.; Kobayashi, N. *Solar Energy Mater. Solar Cells* **2009**, *93*, 2079–2082.
- (26) Granstrom, N.; Petritsch, K.; Arias, A. C.; Lux, A.; Andersson, M. N.; Friend, R. H. *Nature* **1998**, *395*, 257–260.
- (27) Alam, M. M.; Jenekhe, S. A. *Chem. Mater.* **2004**, *16*, 4647–4656.
- (28) Kim, Y.; Cook, S.; Choulis, S. A.; Nelson, J.; Durrant, J. R.; Bradley, D. D. C. *Chem. Mater.* **2004**, *16*, 4812–4818.
- (29) Hou, J.; Tan, Z.; Yan, Y.; He, Y.; Yang, C.; Li, Y. *J. Am. Chem. Soc.* **2006**, *128*, 4911–4916.
- (30) Kim, J. Y.; Lee, K.; Coates, N. E.; Moses, D.; Nguyen, T.-Q.; Dante, M.; Heeger, A. J. *Science* **2007**, *317*, 222–225.
- (31) Zhan, X.; Tan, Z.; Domercq, B.; An, Z.; Zhang, X.; Barlow, S.; Li, Y.; Zhu, D.; Kippelen, B.; Marder, S. R. *J. Am. Chem. Soc.* **2007**, *129*, 7246–7247.
- (32) Pozo-Gonzalo, C.; Pomposo, J. A.; Alduncin, J. A.; Salsamendi, M.; Mikhaleva, A. I.; Krivdin, L. B.; Trofimov, B. A. *Electrochim. Acta* **2007**, *52*, 4784–4791.
- (33) Carrasco, P. M.; Pozo-Gonzalo, C.; Grande, H.; Pomposo, J. A.; Cortazar, M.; Deborde, V.; Hissler, M.; Reau, R. *Polym. Bull.* **2008**, *61*, 713–724.
- (34) Beaujuge, P. M.; Ellinger, S.; Reynolds, J. R. *Nat. Mater.* **2008**, *7*, 795–799.
- (35) Shi, P.; Amb, C. M.; Knott, E. P.; Thompson, E. J.; Liu, D. Y.; Mei, J.; Dyer, A. L.; Reynolds, J. R. *Adv. Mater.* **2010**, *22*, 4949–4953.

- (36) Sonmez, G.; Sonmez, H. B.; Shen, C. K. F.; Wudl, F. *Adv. Mater.* **2004**, *16*, 1905–1908.
- (37) Unur, E.; Beaujuge, P. M.; Ellinger, S.; Jung, J.-H.; Reynolds, J. R. *Chem. Mater.* **2009**, *21*, 5145–5153.
- (38) Unur, E.; Jung, J.-H.; Mortimer, R. J.; Reynolds, J. R. *Chem. Mater.* **2008**, *20*, 2328–2334.
- (39) Takahashi, Y.; Oyaizu, K.; Honda, K.; Nishide, H. *J. Photopolym. Sci. Technol.* **2007**, *20*, 29–34.
- (40) Vasilyeva, S. V.; Unur, E.; Walczak, R. M.; Rinzler, A. G.; Donoghue, E.; Reynolds, J. R. *ACS Appl. Mater. Interfaces* **2009**, *1*, 2288–2297.
- (41) Padilla, J.; Otero, T. F. *Electrochem. Commun.* **2008**, *10*, 1–6.
- (42) Reeves, B. D.; Grenier, C. R. G.; Argun, A. A.; Cirpan, A.; McCarley, T. D.; Reynolds, J. R. *Macromolecules* **2004**, *37*, 7559–7569.
- (43) Nielsen, C. B.; Angerhofer, A.; Abboud, K. A.; Reynolds, J. R. *J. Am. Chem. Soc.* **2008**, *130*, 9734–9746.
- (44) Kumar, A.; Welsh, D. M.; Morvant, M. C.; Piroux, F.; Abboud, K. A.; Reynolds, J. R. *Chem. Mater.* **1998**, *10*, 896–902.
- (45) Mortimer, R. J.; Graham, K. R.; Grenier, C. R. G.; Reynolds, J. R. *ACS Appl. Mater. Interfaces* **2009**, *1*, 2269–2276.
- (46) Gaupp, C. L.; Welsh, D. M.; Rauh, D. R.; Reynolds, J. R. *Chem. Mater.* **2002**, *14*, 3964–3970.
- (47) Berns, R. S. *Billmeyer and Saltzman's Principles of Color Technology*, 3rd ed.; John Wiley & Sons, Inc.: New York, 2000.